Nuclear Materials and Energy 12 (2017) 1363–1367

Contents lists available at ScienceDirect

Nuclear Materials and Energy

journal homepage: www.elsevier.com/locate/nme

Smart alloys for a future fusion power plant: First studies under stationary plasma load and in accidental conditions

A. Litnovsky[a,*], T. Wegener[a], F. Klein[a], Ch. Linsmeier[a], M. Rasinski[a], A. Kreter[a], B. Unterberg[a], M. Vogel[a], S. Kraus[a], U. Breuer[b], C. Garcia-Rosales[c], A. Calvo[c], N. Ordas[c]

[a] Forschungszentrum Jülich GmbH, Institut für Energie- und Klimaforschung – Plasmaphysik, Partner of the Trilateral Euregio Cluster (TEC), 52425 Jülich, Germany
[b] Forschungszentrum Jülich GmbH, Central Institute for Engineering, Electronics and Analytics ZEA-3, 52425 Jülich, Germany
[c] CEIT-IK4 Technology Center and Tecnun (University of Navarra), E-20018 San Sebastian, Spain

ARTICLE INFO

Article history:
Received 14 July 2016
Revised 19 October 2016
Accepted 17 November 2016
Available online 24 December 2016

Keywords:
DEMO
Advanced plasma-facing materials
Smart tungsten alloys
Suppressed oxidation
Plasma sputtering
Accidental conditions

ABSTRACT

In case of an accident in the future fusion power plant like DEMO, the loss-of-coolant may happen simultaneously with air ingress into the vacuum vessel. The radioactive tungsten and its isotopes from the first wall may become oxidized and vaporized into the environment. The so-called "smart" alloys are under development to suppress the mobilization of oxidized tungsten. Smart alloys are aimed at adjusting their properties to environment. During regular operation, the preferential sputtering of alloying elements by plasma ions should leave almost pure tungsten surface facing the plasma. Under accidental conditions, the alloying elements in the bulk will form an oxide layer protecting tungsten from mobilization.

The first direct comparative test of pure tungsten and smart alloys under identical plasma conditions was performed. Tungsten–chromium–titanium alloys were exposed simultaneously with tungsten samples to stationary deuterium plasma in linear plasma device PSI-2. The ion energy and the temperature of samples corresponded well the conditions at the first wall in DEMO. The accumulated fluence was 1.3 $\times$ 10^{26} ion/m^2. The weight loss of pure tungsten samples after exposure was Δm_W = 1000–1150 µg. The measured weight loss of sputtered smart alloy sample Δm_{SA} = 1240µg corresponds very well to that of pure tungsten providing experimental evidence of good resistance of smart alloys to plasma sputtering.

Plasma exposure was followed by the oxidation of alloys at 1000 °C accomplishing the first test of these new materials both in a plasma environment and under accidental conditions. Compared to pure tungsten, smart alloys featured the 3-fold suppression of oxidation. Plasma exposure did not affect the oxidation resistance of smart alloys. At the same time, the self-passivation of the protective layer did not occur, calling for further optimization of alloys.

Introduction and motivation

In future fusion power plant like DEMO, the in-vessel components will be subjected to the unprecedented steady-state particle and neutron loads. Currently envisaged materials for fusion reactor experiments will face the challenge of the rapidly degrading performance in the power plant [1]. Presently, tungsten is deemed as the best-suited plasma facing material for the first wall of DEMO. Tungsten features low fusion fuel retention, low sputtering by plasma ions and perfect thermal conductivity at elevated temperatures. However in the case of an accident in fusion power plant, the application of tungsten could be questionable. During the so-called loss-of-coolant accident (LOCA) combined with an air ingress, the tungsten plasma-facing components (PFCs) will be heated up to 1000 °C–1200 °C due to nuclear decay heat [2]. Such an elevated temperature will remain for months at the absence of an active cooling. At such a temperature the radioactive tungsten and its isotopes will form volatile oxides, which can be then mobilized into atmosphere with the rates 10–100 kg per hour. Therefore, the oxidation of tungsten must be suppressed at the maximum possible extent.

New advanced tungsten-based so-called "smart alloys" represent an attractive option for providing the intrinsic safety to the fusion power plant. These materials possess the capability of adjusting their properties according to environment. During the routine plasma operation in the power plant, the first few nanometers

* Corresponding author.
E-mail address: a.litnovsky@fz-juelich.de (A. Litnovsky).

http://dx.doi.org/10.1016/j.nme.2016.11.015

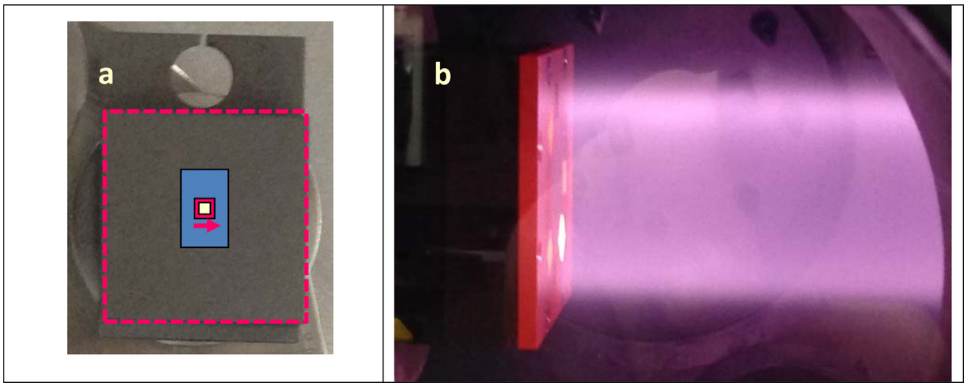

Fig. 1. Smart alloys and tungsten samples: (a) a view of a typical sample with the measurement locations: arrow **shows** the location of surface roughness scan with stylus profiler, large area is the location of SEM surveys, smaller square in the middle is the location of SIMS depth profiles and the smallest square shows the location of FIB cut and (b) Exposure of smart alloys and pure tungsten samples in steady-state deuterium plasma of PSI 2 linear device. A side view to the heated tungsten and smart alloy samples mounted into the holder and glowing during plasma exposure is presented.

of the surface will be sputtered by the plasma ions. The lighter alloying elements will be sputtered earlier, leaving almost a pure tungsten surface facing the plasma. In the case of an accident however, the alloying elements in the bulk of the smart alloy will react with oxygen and create their own stable oxides to protect tungsten from mobilization.

There are severe constraints in the choice of possible alloying materials. The candidate materials should:

- Have low activation, at least comparable to that of tungsten.
- Form stable, well adhesive hard-melting oxides.
- Allow the suppression of oxidation without significant volume increase.

The development of self-passivating tungsten alloys and oxidation tests of their performance under accidental conditions was reported in [3–7]. However, besides the suppressed oxidation, new materials need to be qualified under plasma exposure. The first results of such a plasma exposure along with the subsequent oxidation of exposed tungsten and smart alloy samples are reported in this paper.

Manufacture of smart alloy, pre-characterization and plasma exposure

The W–Cr–Ti smart alloy samples were produced at CEIT (Spain) from elemental tungsten, chromium and titanium powders mechanically alloyed using the planetary ball mill with tungsten carbide vials and milling balls. The alloyed powder was encapsulated and underwent hot isostatic pressing (HIP) at 1200 °C at the pressure of 150 MPa in argon atmosphere. Manufactured bulk material featured nanocrystalline tungsten grains of about 90–110 nm and contained 10 wt% of Cr, 2 wt% of Ti and the rest of W. Details of the manufacturing process and the initial characterization of manufactured materials are provided in [8]. The ingot of the W–Cr–Ti smart alloy was delivered to Forschungszentrum Jülich (FZJ) where samples were produced out of this material using the spark erosion following the standard methods for tungsten processing without any changes made specifically for smart alloys. The samples had dimensions of 10 × 10 mm and 10 × 15 mm with the thickness of 3 and 3.5 mm respectively. Samples were mechanically ground to remove the rest deposits remaining from spark erosion cutting. Both tungsten and smart alloy samples were characterized before the plasma exposure. The total weight of the sample was measured using Sartorius MSA225P micro balance with an accuracy of 10 µg in the MirrorLab [9]. Surface roughness R_a was evaluated using the stylus profiler Dektak 6 M from Bruker. Scan locations are shown in Fig. 1(a). Each scan of surface roughness consisted from five to seven measurements, the final result was averaged.

Time-of-flight Secondary Ion Mass-Spectrometry (ToF SIMS) investigations were made in the middle of each sample using ToF-SIMS IV (IONTOF GmbH, Münster, Germany) facility on locations shown in Fig 1(a). SIMS measurements provided a depth profiling of the elemental composition of all samples. The investigations were made with both 2 keV Cs^+ sputter ions for better sensitivity for non-metallic elements and oxides and with 2 keV O_2^+ ions for better sensitivity for metals.

Scanning electron microscopy (SEM) surface surveys were made on each sample on the area shown in Fig. 1(a) using the Carl Zeiss CrossBeam XB 540 microscope equipped with the focused ion beam (FIB). Cross-section viewing by FIB was performed in the central area of each sample shown with the smallest square in Fig. 1(a). Special markers were made with an ion beam on the side surface of each FIB crater. The distance between the two neighboring markers corresponded to 1 µm. The markers were used to directly measure the material sputtered during plasma exposure.

The pre-characterized samples were installed to the designed sample holder and exposed to steady-state deuterium plasma in linear plasma device PSI-2 [10]. For all samples, an area of 10 × 10 mm was directly exposed to plasma. The photo of the samples during the plasma exposure is shown in Fig. 1(b). During exposure plasma parameters were monitored using the moveable Langmuir probe. The measured electron temperature was 30-35 eV, the plasma density was $N_e \sim 7 \times 10^{11}$ ion/cm^3. The measured ion flux was 1×10^{18} D/(cm^2 × s). Samples were biased at −250 V, the resulting ion energy was about 220 eV, providing the conservative upper boundary for ion sputtering expected for DEMO in [11]. The temperature of the samples was controlled via thermocouple mounted behind the sample and using the infrared camera FLIR SC7500. During the exposure the temperature of samples was ranging from 576 °C to 715 °C as provided in Table 1, matching well the expected temperature of the first wall in DEMO [11]. Apart from the fact, that such temperatures are not affecting the sputtering coefficients, temperatures for the pairs of samples W1-SA1 and W2-SA2 correlate fairly well, providing an evidence of identical plasma conditions for these pairs of samples. The total duration of the exposure was 3.6 h, the total accumulated fluence was estimated to be 1.3×10^{26} D/cm^2.

Results of exposure and analysis

After the exposure the samples were weighed. For exposed tungsten sample W1 a mass loss of 1000 µg was measured, tung-

Table 1
Characteristics of tungsten and smart alloy samples during and after plasma exposure.

Sample	Temperature during exposure, °C	Weight loss during exposure, μg	Roughness R_a before exposure, nm	Roughness R_a after exposure, nm
W1	702	1000	215	255
W2	665	1150	232	324
SA1	715	1240	690	377
SA2	576	N.a.	500	N.a.

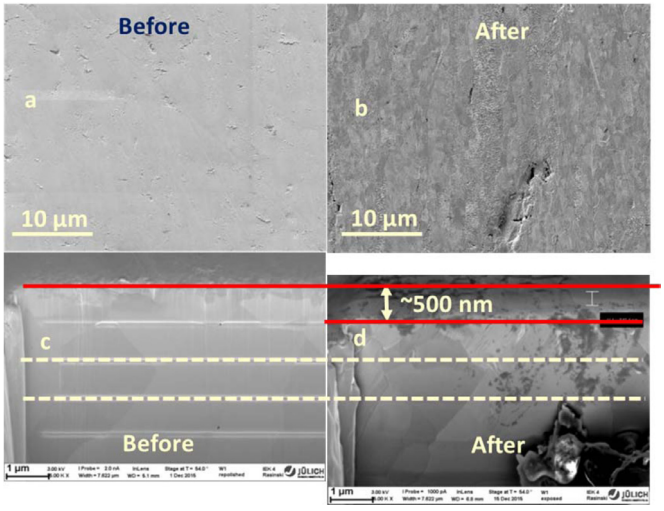

Fig. 2. Surface morphology and cross-section viewing of pure tungsten sample before and after exposure to steady-state deuterium plasma: (a) top surface before exposure, (b) top surface after exposure, (c) cross-section viewing before exposure and (d) cross section viewing after exposure. The FIB labels are marked on Fig. 2(c) with the dashed lines. The thickness of removed layer is shown on Fig. 2(d).

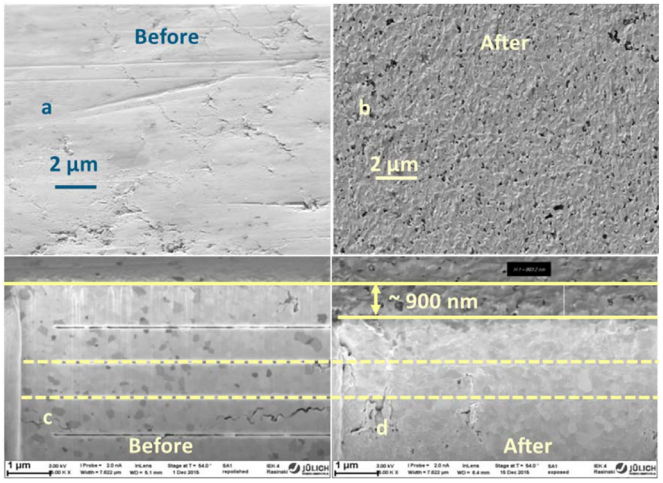

Fig. 3. Surface morphology and cross-section viewing of smart alloy sample before and after exposure to steady-state deuterium plasma: (a) top surface before exposure, (b) top surface after exposure, (c) cross-section viewing before exposure and (d) cross section viewing after exposure. The FIB labels are marked on Fig. 3(c) with dashed lines. The thickness of removed layer is shown on Fig. 3(d).

sten sample W2 exhibited the mass loss of 1150 μg as provided in the Table 1. The decrease of the mass loss of exposed smart alloy SA1 sample was measured to be 1240 μg. The exposed area of all samples was 1 cm^2. Measured mass loss of tungsten was used to estimate the experimental sputtering rate for this material. The attained sputtering yield of 2.4×10^{-4} at/ion corresponds well to the experimental data provided in [12] however, it is a bit higher than that expected from theory [13,14]. The reason for more effective erosion in plasma of PSI 2 linear device may be attributed to the small 0.1% fraction of oxygen in plasma. The calculated removal of material by sputtering from the mass loss measurements was estimated to be: 500 nm for tungsten and about 800 nm for a smart alloy.

The sputtered depth was measured directly using the craters pre-marked with the focused ion beam as described earlier. The comparison of the cross-section viewing before and after exposure is provided on Fig. 2 for pure tungsten sample W1 and on Fig. 3 for smart alloy SA1. The removed amount of material due to sputtering from the weight loss measurements was compared for tungsten with the value measured using FIB crater. The expected loss of tungsten was 500 nm, whereas the direct measurements showed 560 nm outlining the perfect correlation between weight loss and direct measurements of sputtered material. The measured material removal from the smart alloy sample was about 900 nm which is in a very good correlation with the weight loss measurements.

Surface morphology of all the samples was investigated with SEM microscope before and after exposure. The respective SEM photos can be found in Fig. 2 for tungsten sample W1 and on Fig. 3 for the smart alloy sample SA1. Observations show the slight morphology changes under the ion bombardment. On the surface of the smart alloy some hole-like structures with the size less than 500 nm have been detected. Most probably, these structures were formed on locations of alloying elements sputtered by plasma ions.

Surface roughness was measured in the middle of all samples after exposure in PSI 2 on the locations shown in Fig 1(a). The results of surface roughness measurements are presented in Table 1. A slight increase of surface roughness from 215 to 255 nm for sample W1 and from 232 to 324 nm for tungsten sample W2 was detected. Such an increase of roughness can be due sputtering of polycrystalline tungsten by plasma ions. Differently oriented grains of a polycrystalline material are sputtered with the different efficiency leading to the increase of surface roughness. The impact of plasma exposure on surface roughness of smart alloy is more surprising at a first glance. The initially high roughness of the sample SA1 of 690 nm decreased down to 377 nm – a value similar to that measured on pure tungsten samples. The observed effect can be described by the initial fast sputtering of the lighter alloying elements having higher efficiency of sputtering by plasma ions. The depleted surface contains almost pure tungsten and its evolution becomes similar to that of pure tungsten sample. The measured material removed from the smart alloy sample during plasma exposure is 900 nm which already exceeds the initial surface roughness value. This finding implies that the final surface morphology after plasma exposure is dominated mostly by the plasma sputtering and not by initial surface roughness.

The evidence of such a preferential sputtering of alloying elements was provided by the dedicated SIMS measurements made on all samples on locations shown on Fig 1(a). Prior to exposure, all smart alloy samples featured the homogeneous distribution of tungsten and alloying elements along the bulk of the sample. The example of the SIMS depth profile measured on the sample SA1 after the plasma exposure is shown in Fig. 4. Concentrations of tungsten (W) as well as alloying materials (Cr and Ti) are plotted

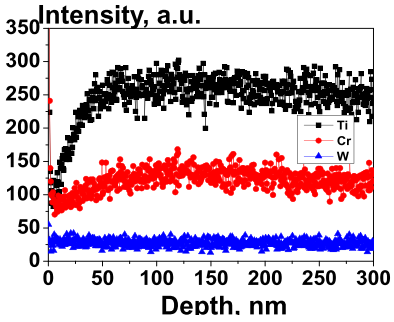

Fig. 4. The distribution of tungsten and alloying elements in the depth of the smart alloy sample after plasma exposure.

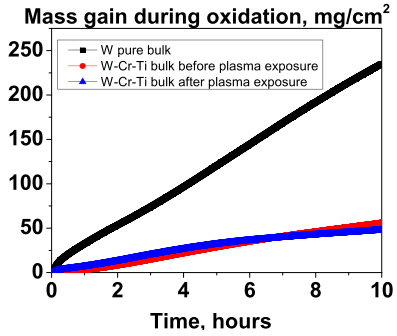

Fig. 5. Mass gain caused by the oxidation of the pure tungsten and W–Cr–Ti smart alloys.

along the depth of the sample. As it can be inferred from the depth distributions, tungsten material matrix remains almost unchanged during the exposure whereas Cr and Ti fractions are depleted at the surface till the depth of ~50 nm and reach the stationary values only at the depth >75 nm. These results support our initial expectation of preferential sputtering of alloying elements and can explain the observed increasing similarity of the surface roughness of smart alloys and pure tungsten samples reported above.

Thermo-oxidation of tungsten samples and smart alloys

In order to study the effect of plasma exposure on oxidation properties of smart alloys, series of thermo-oxidation studies were performed after plasma exposure. Thermo-oxidation studies were performed in the newly built ThermoLab at the FZJ using the symmetrical double-oven thermogravimetric (TGA) facility KEP Setaram TAG 16. The characteristic feature of this TGA facility is the double-oven system providing low-noise reliable the measurements.

During the thermo-oxidation measurements, the samples were placed in highly controlled and well characterized synthetic air atmosphere containing 80 vol% N_2 and 20 vol% O_2 at 1 atmosphere and oxidized isothermally at the temperature 1000 °C for ten hours. The choice of temperature corresponds to the expected value during the accident on the fusion power plant. The samples were exposed under identical conditions. During the thermo-oxidation tests the mass gain due to oxide formation occurs. The mass gain may turn to a mass loss, if the sample experiences failure, as e.g. delamination or evaporation. The mass change was measured during the exposure of samples with the precision better than 0.1 μg.

Three samples were chosen for thermo-oxidation tests: pure tungsten sample, manufactured and rolled according to the ITER specifications, smart alloy which were never exposed to plasma and smart alloy after plasma exposure. The resulting dependencies are presented in Fig. 5 as the mass gain over time. Pure tungsten sample is remarkable for the by far highest linear oxidation rate of 6×10^{-3} mg/(cm^2 × s). Smart alloys feature the significant suppression of oxidation: the measured oxidation rate of 2×10^{-3} mg/(cm^2 × s) was detected for W–Cr–Ti smart alloy systems both exposed and non-exposed to plasma. The same oxidation behavior of smart alloys confirms our expectations that plasma exposure does not have any negative effect on oxidation advantages of smart alloys.

At the same time, the mass gain during the oxidation is linearly proportional to time for all studied systems. Whereas expected for the pure tungsten samples, this result means that the suppression of oxidation in the studied smart alloys is not yet accompanied with self-passivation of protecting oxide film. Should this happen, the oxidation would follow diffusion-driven parabolic dependence on time. This finding outlines explicitly the need in future optimization of smart alloys despite of significant advantageous suppression of tungsten oxidation already detected in the course of present studies.

Summary and outlook

The bulk advanced W–Cr–Ti smart alloys with the suppressed oxidation became manufactured using mechanical alloying followed by HIP procedure described above. Smart alloy samples were machined with conventional tools used for tungsten processing without any modifications of tooling or machining procedures.

For direct comparison, the data is provided for smart alloy sample previously exposed to plasma as well as for the sample that not experienced plasma exposure.

First direct comparative plasma test of advanced smart tungsten-based alloys and pure tungsten samples was made under conditions expected at the first wall in DEMO. Exposed under identical plasma conditions, tungsten and smart alloy samples demonstrated similar sputtering under plasma ion bombardment in the PSI 2 linear device. Only a moderate change of surface morphology was detected after exposure despite of 500 nm of removed material for tungsten samples and about 900 nm of material removed from smart alloys. At the same time, the expected preferential sputtering of alloying elements during the plasma exposure of smart alloys was confirmed experimentally. The final surface roughness of smart alloys after plasma exposure was similar to that of pure tungsten samples. Controlled oxidation of smart alloys did not reveal any negative effect of plasma exposure on the suppressed oxidation. Both exposed and non-exposed smart alloys featured the 3-fold suppression of the oxidation as compared to pure tungsten. These findings outline promising features of new advanced tungsten – based materials for the use in future fusion power plants and call for continuation of this promising study. At the same time, despite of significant suppression of tungsten mobilization, the self-passivation of the protective oxide layer was not yet achieved calling for further optimization of the smart alloys.

New yttrium-containing tungsten smart alloys became available recently. The new W–Cr–Y systems feature more effective long-term suppression of tungsten oxidation coupled with better long-term stability of protective layers. The plasma tests of these innovative new smart alloys are in preparation. The sputtering of new smart alloys by plasma, corresponding surface changes and the deuterium retention in the exposed samples is in focus of future research. The combined full working cycle test including plasma and oxidation testing of new systems is of prime importance. Future studies will be carried out to optimize the overall performance of smart alloys including further suppression of oxidation by self-passivation and investigations of deuterium inventory. Dedicated efforts will be made on optimization of thermo-mechanical

properties of smart alloys such as thermal conductivity, hardness and ductile-to-brittle transition temperature.

Acknowledgments

The author would like to express the sincere gratitude to our colleagues from the Central Institute of Engineering, Electronics and Analytics of the Forschungszentrum Jülich: to Mr. A. Schwaitzer for help and advices on sample holders and to Mr. K.-H. Junglas for organizing the machining of smart alloy and tungsten samples. We are grateful to Mr. J. Faupel for a fast and efficient commissioning and support of our thermogravimetric facility. A part of these studies has been carried out within the framework of the EUROfusion Consortium and has received funding from the Euratom Research and Training Programme 2014–2018 under grant agreement no. 633053. The views and opinions expressed herein do not necessarily reflect those of the European Commission.

References

[1] J.W. Coenen, S. Antusch, M. Aumann, et al., Phys. Scr. 167 (2016) 014002.
[2] D. Maisonnier et al., A Conceptual Study of Commercial Fusion Power Plants, Final Report, 2005, EFDA; EFDA-RP-RE-5.0.
[3] F. Koch, H. Bolt, Phys. Scr. T128 (2007) 100.
[4] F. Koch, S. Köppl, H. Bolt, J. Nucl. Mater. 386–388 (2009) 572–574.
[5] F. Koch, J. Brinkmann, S. Lindig, T.P. Mishra, C. Linsmeier, Phys. Scr. T145 (2011) 014019.
[6] P. López-Ruiz, N N. Ordás, S. Linding, et al., Phys. Scr. T145 (2011) 014018.
[7] C. García-Rosales, P. López-Ruiz, S. Alvarez-Martín, A. Calvo, N. Ordás, F. Koch, J. Brinkmann, Fusion Eng. Des. 89 (2014) 1611–1616.
[8] A. Calvo, C. García-Rosales, F. Koch, Manufacturing and testing of self-passivating tungsten alloys of different composition, Nucl. Mater. Energy (2016). http://dx.doi.org/10.1016/j.nme.2016.06.002.
[9] MirrorLab Website (https://tec.ipp.kfa-juelich.de/mirrorlab/), Access details: https://mirrorlab@fz-juelich.de.
[10] A. Kreter, C. Brandt, A. Huber, Fusion Sci. Technol. 68 (8) (2015).
[11] Yu. Igitkhanov, B. Bazylev, I. Landman, R. Fetzer, KIT Scientific report 7637 (2013) 20.
[12] W. Eckstein, C. Garcia-Rosales, J. Roth, W. Ottenberger, “Sputtering data”, IPP Garching Report 9/82 (1993) 116.
[13] W. Eckstein, “Calculated sputtering, reflection and range values”, IPP Garching Report 9/132 (2002) 211.
[14] W. Eckstein, “Sputtering yields” in “Sputtering by particle bombardment: Experiments and Computer Calculations from Threshold to MeV Energies”, in: R. Behrisch, W. Eckstein (Eds.), Springer, Berlin, 2007.